BOLETÍN DE LOS OBSERVATORIOS DE TONANTZINTLA Y TACUBAYA, VOL. 4, N°27, 1965.

THE CONTINUUM EMISSION OF THE ORION NEBULA

Manuel E. Méndez

SUMARIO

El continuo de la región más brillante de la Nebulosa de Orion ha sido observado fotoeléctricamente. El rango espectral cubierto va desde λ 3500 hasta λ 11000. Las contribuciones al continuo producidas por diferentes procesos ha sido analizada. La componente, asociada a la dispersión electrónica, se ha calculado utilizando observaciones del continuo de las estrellas del Trapezio. Esta contribución es apreciable y es la responsable de la polarización detectada en la Nebulosa. La luz estelar es dispersada por polvo dando otra componente del continuo nebular; esta última ha sido empleada para derivar el albedo del material sólido; la variación del albedo con la longitud de onda ha permitido estimar el índice de refracción.

ABSTRACT

The continuum produced by the brightest region of the Orion Nebula has been observed photoelectrically. The spectral range covered is from λ 3500 to λ 11000. The various processes contributing to the continuum energy have been studied. The component provided by electron scattering has been computed, using the observed continuum of the Trapezium stars. This contribution is quite significant and it is responsible for the polarization found in the Nebula. The stellar light is also scattered by dust giving some contribution to the continuum energy. From the latter component the albedo of the solid has been derived. The variation of the albedo with wavelength has permitted to estimate the value of the refractive index.

© Copyright 1965: Observatorio Astronómico Nacional, Universidad Nacional Autónoma de México

I. Introduction

The atomic processes which produce continuum emission by radiative recombination have been the subject of extensive theoretical investigations. In particular, the problem of the hydrogen and helium continua has been worked out to a high degree of precision. The contribution to the continuum by these two elements can thus be computed quite accurately for the physical conditions prevailing in the Orion Nebula. Therefore, a direct comparison of the theoretical results obtained in this way, with the observations of this object, should provide very useful information about the nature of the other possible mechanisms, which might make significant contributions to the continuum spectrum of the Nebula. By this method, one can directly study the behavior of the solid particles imbedded in that region. For instance, knowledge of the particle albedo, which can be readily derived, is very important if one desires to obtain information about the electric properties of the solid matter present in the Orion Nebula. Moreover, it is well known that polarization has been detected in the brightest regions of the Nebula. Electron scattering might be the most effective agent in producing the polarization which is important because the variation of polarization with both position and wavelength can be used to investigate the relative geometry of stars and gas.

In comparison with line intensity measures, the Orion Nebula continuum spectrum has been seldom observed. The energy distribution in the nebular continuum has been measured both in the blue, (Barbier, 1944; Greenstein 1964), and in the red (Andrillat and Andrillat, 1959). But these observations were carried out photographically. More recently, Reitmeyer (1965) has observed the Nebula, photoelectrically using interference filters. However, the past observers have not taken in account the proper correction for interstellar reddening; as a consequence, incorrect conclusions have been derived.

II. The observations

In the present investigation the spectral range from λ 3400 to λ 11000 was covered using two photoelectric cells. The 1P21 was used to measure the region from λ 3400 to λ 5700. Whereas a RCA 7102 was employed for longer wavelengths with the Ebert scanning spectrometer at the Cassegrain focus of the 60-inch telescope at the Mount Wilson Observatory. These observations have been already described. (Méndez 1964, 1965), and only a review will be given here. A 600 lines/mm. grating blazed at λ 3500, in the second order, is the dispersive element. With the red cell —RCA 7102— the first order is employed, the dispersion being 20 A/mm. The overlapping second order was cut off by an amber filter. When the second order is in operation, the blue cell is used, the dispersion being 10 A/mm. Here a yellow KZ filter is required for λ larger than 4600, to cut off the UV of the third order.

Two types of observations were obtained: the bright region, about 45 seconds of arc away from Θ′ Ori, was selected to study the nebular continuum; and the Trapezium, as a whole, was also observed.

While the nebular continuum was recorded from λ 3500 to λ 11000, the four stars of the Trapezium were recorded with the blue cell only, covering the spectral range from λ 3400 to λ 6000. Ac-

count was taken of the contribution to the continuum integrated star light produced by the nebula, by substracting the energy flux observed at the nebular bright region.

The nebular region was observed using a diaphragm of 14" in diameter, which corresponds to a projected distance, on the nebula, of 0.0315 pc.

The observations were calibrated using three standard stars of the list given by Oke (1964): they are ε Ori, α Leo and γ Gem.

TABLE 1*

λ	A *Trapezium*	A *Nebular region*	ΔA
3400	2.74	2.33	0.41
3650	2.58	2.19	0.39
3860	2.46	2.09	0.37
4190	2.30	1.95	0.35
4590	2.14	1.82	0.32
5060	1.96	1.67	0.29
5560	1.83	1.55	0.28
5810	1.78	1.51	0.27
6050	1.72	1.46	0.26
6670	1.61	1.36	0.25
7460	1.50	1.27	0.23
8000	1.42	1.20	0.22
8750	1.35	1.14	0.21
10000	1.21	1.03	0.19
10870	1.13	0.96	0.17

* A in magnitudes.

III. The Reddening Correction

Multicolor photometry of the Trapezium stars was used in the past to correct the nebular observations for interstellar extinction. However, it has been shown that a more direct correction can be obtained if one uses the Paschen and Balmer lines; by this method, a reddening curve has been obtained for the bright nebular region (Mendez, 1965). The Trapezium stars have a different amount of effective reddening than the nebular light, the absorption at the center of the nebula being larger. Table 1 gives the values of the absolute absorption at various wavelengths, for both the Trapezium and the nebular region.

The absorption suffered by the exciting stars was derived using the value of 4.8 for R, the ratio of the absorption, at the effective wavelength of the V filter, to the mean color excess in B-V. From the data given in Table 1, one may consider that the light coming from the stars to the bright nebular region is reddened by an amount equal to the difference between columns 2 and 3, and also given in column 4. That is, the Trapezium stars (assumed to be at the center) as seen from the bright nebular region under discussion, look much less reddened than as seen from the earth. Although this tacit assumption might not be altogether justified, it will be used here as a good working hypothesis.

With the values of the absorption thus determined, one can now directly obtain the stellar fluxes at different positions. In particular, two regions are important: the Trapezium itself, and the bright patch of nebulosity observed. Table 2 provides the fluxes in absolute units, per interval of 1 Å centered at the wavelength indicated.

The spectrophotometric data from Table 2 can be used to derive the color temperature of the Trapezium stars as a whole. At the wavelength of λ 4250, the value of the absolute gradient,

$$\varphi_\lambda = 5\bar{\lambda} - \frac{d F_\lambda}{d\,(1/\lambda)} \qquad (1)$$

is 0.55, for the unreddened energy distribution; the corresponding value for the continuum distribution, as observed directly at the Earth, is 1.28. From these resulting numbers, the color temperatures are 58 500 °K and 11 900 °K, respectively. The latter is in good agreement with the value of 12 400

© Copyright 1965: Observatorio Astronómico Nacional, Universidad Nacional Autónoma de México

°K, obtained by Greenstein (1946). The unreddened color temperature is nearly equal to that of an 05 star, as given by Barbier and Chalonge (1940).

TABLE 2

Stellar fluxes of energy in units of 10^{-11} erg cm^{-3} sec^{-1} A^{-1}

λ	*As seen at the earth*		*As seen at the* observed nebulosity*
	Reddened	*Unreddened*	
5810	4.55	23.2	5.84
5560	5.09	27.1	6.61
4590	7.65	54.7	10.27
4190	9.14	76.0	12.62
4040	10.03	99.6	13.71
3860	10.81	104.2	15.18
3650	11.70	125.8	16.75
3400	13.52	168.3	19.84

* *if it were at the earth-nebula distance.*

IV. The Sources of Continuum Emission

For an emission nebula, there exist five possible mechanisms, which produce a continuum and are:

1) Radiative recombination of ionized atoms Obviously, only hydrogen and helium are important.
2) Free-free emission.
3) Two photon emission. Only H is important in the observable spectral region.
4) Thomson Scattering of star light by free electrons.
5) Scattering of stellar light by dust particles.

Processes 1 and 2 can be computed directly and no further comments are needed. Although for process number three, the rate of emission is given by the theory of radiative recombination, some doubts have arisen in the past about whether or not the Ly-α photons, by electron collision with the hydrogen atoms in the 2s state, would be degraded to two continuum photons of lower energy. This possibility can be ruled out as a result of the following general considerations. The number of Ly-α photons produced per unit volume is given by $(1-x)\ \alpha_B\ N_e^2$; where α_B is the total recombination coefficient, (Seaton 1960); x, of the order of 0.34, is the fraction of the electron population of the second state for which $l = 0$; and N_e is the electron density. Since an average Ly-α quantum is scattered Q times before it leaves the nebula, the rate of the 2p to 2s collisional deexcitation is:

$$H = 0.91\ (1-X)\ \alpha_B\ N_e^2\ \frac{<\sigma V>_{2p-2s}}{A_{2p\,1s}}\ N_e\ Q \qquad (2)$$

the factor 0.91 comes from the He/H abundance ratio, (Méndez 1964). $<\sigma V>_{2p-2s} N_e$ gives the collisional rate and $A_{2p\,1s}$ is the spontaneous radiative transition probability.

Therefore, the energy emitted by the two-photon emission process, including the contributions of electrons recombining into the 2s level, is:

$$E_{2q} = 0.91 N_e^2\ [0.66\ \alpha_B\ \frac{<\sigma V>_{2p-2s}}{A_{2p\,1s}}\ N_e\ Q + \gamma_o\ (2q)\ ]\ d\,(h\nu) \qquad (3)$$

here $\gamma_o(2q)$ is the continuum recombination coefficient for the two-photon emission process. For the observed nebular region, one can adopt $N_e = 10^4$ cm^{-3}. The value of Q is about 8×10^5, for a dust free nebula (Osterbrock 1962). Therefore, the first term in the bracket is, for $T_e = 10^4$ °K, equal to 3.8×10^{-16}. This value must still be decreased by at least a factor of 25 due to the dust extinction of the Ly-α radiation. Since the $\gamma_o(2q)$ coefficient is always of the order of 10^{-14}, one can safely conclude that the Ly-α quanta in the nebula cannot produce a significant amount of two photon emission.

© Copyright 1965: Observatorio Astronómico Nacional, Universidad Nacional Autónoma de México

Moreover, the intensity of the two-quantum continuum is reduced due to collisional 2s – 2p transitions, produced by proton impacts. This rate has been accurately computed by Seaton (1955), and as a result the new coefficient is given by

$$\gamma\,(2q) \;=\; \frac{\gamma_e\,(2q)}{1 \,+\, 6 \times 10^{-5}\,N_e} \qquad (4)$$

Therefore, the three first processes combined can be represented by the expression

$$E_e \;=\; \frac{91\,N^2{}_e\,[\gamma\,(H^+) \,+\, 0.1\;\gamma\,(H_e{}^+) \,+\, \gamma\,(2q)\,]\,dh\nu}{0.91\,N^2{}_e\;\alpha_{4,2}\;(T_e)\;h\nu_\beta} \qquad (5)$$

which is in units of intensity of H_β; that is, $I\,(H_\beta)$ is taken as 100. In equation (5), $\gamma(H^+)$ represents the continuous coefficient for free transitions plus recombination, $\gamma(He^+)$ is the corresponding value for recombination of the He II atoms. Putting E_e in units of wavelength interval, and after some manipulation:

$$E_e \;=\; 1.62 \;\times\; 10^{15}\;\lambda^{-2}\;[0.1\;\gamma\,(He^+) \;+\; \gamma\,(H^+) \;+\; \gamma\,(2q)\,]\;\Delta\lambda \qquad (6)$$

Here λ and $\Delta\lambda$ are both in microns. The values for the γ's have been tabulated by Seaton (1960) for various temperatures. The band width, $\Delta\lambda$, used in the observations was 10 Å. Adopting $N_e = 10^4$ cm^{-3}, calculations have been carried out for some values of λ. The results are compared with some selected observed values in Table 3. The latter numbers were chosen according to the curve fitted to the observed values, as shown in Figure 1. The observed value at λ 3650– was measured photographically; the photoelectric value is higher (10.4), but is was determined at λ 3500.

The difference between the two values is also given in Table 3. These numbers represent the continuum energy produced by the other two processes, namely, electron scattering and the scattering of stellar light by solid particles. The contribution of process number 4 must be obtained first.

TABLE 3

λ	E_{Theory}	E_{obs}	ΔE
3650–	6.25	8.64	2.39
3650+	0.88	2.75	1.87
4200	0.90	2.26	1.36
5000	0.90	1.65	0.55
5700–	0.87	1.30	0.43
5700+	0.67	1.30	0.63
7398	0.56	0.96	0.30
8192–	0.59	0.95	0.36
8192+	0.27	0.70	0.43
9115	0.25	0.64	0.39
10000	0.24	0.57	0.33

As it is well known, stellar light, which is initially unpolarized, is scattered by electrons. The amount of radiation scattered by each electron, into a solid angle $\Delta\Omega$, in a direction making an angle Θ with the direction of incidence is given by the relation

$$I_s \;=\; \frac{8\pi}{3}\left(\frac{e^2}{mc^2}\right)^2 I_T\;\Delta\Omega\left[\frac{3}{4}\;(1 \;+\; cos^2\;\Theta)\;\frac{\Delta\Omega'}{4\pi}\right] \qquad (7)$$

where the factor in the brackets is the probability of scattering within an angle $\Delta\Omega'$. The value of the intensity I_T, can be derived from the data of the fourth column of Table 2, and with the value of the area covered by the scanner diaphragm. If the four stars of the Trapezium are taken as a point source, the flux received at the Earth will be.

$$F_s \;=\; 0.64 \;\times\; 10^{-24}\;N_e\;L\;I_T\;\Delta\Omega' \qquad (8)$$

where L is the path length along which the stellar light is dispersed by electrons; this length will be taken as ⅓ parsec. Since it is clear from Table 3 (beyond λ 5700) that ΔE is almost independent of

© Copyright 1965: Observatorio Astronómico Nacional, Universidad Nacional Autónoma de México

wavelength, and close to 0.38 the value of N_e is fixed in such a way that the flux at λ 5700, in a 10 Å interval, is about 0.38. Although this procedure is not completely justified, the error introduced can not exceed 0.10 in the same units. The flux at H_β has been already derived from surface brightness measurements, and when it is corrected for extinction one obtains, for the observed region, (Méndez 1965),

$$F\ (H_\beta) = 6.35 \times 10^{-10}\ erg\ cm^{-2}\ sec^{-1}.$$

The resulting electron density is then equal to 4500 a value in good agreement with the maximum projected electron density, as derived by the [OII] lines, multiplied by a condensation factor of about ⅓, (Méndez 1965, Peimbert 1962). Using the values of Table 2 and 4, one can directly compute the contribution to the energy in the nebular continuum produced by the stellar light, after scattering by solid particles. Table 4 gives the results, and Figure 1 shows the distribution of the light scattered by dust, as a function of wavelength. The color temperature for the dust continuum is close to 12 600 °K.

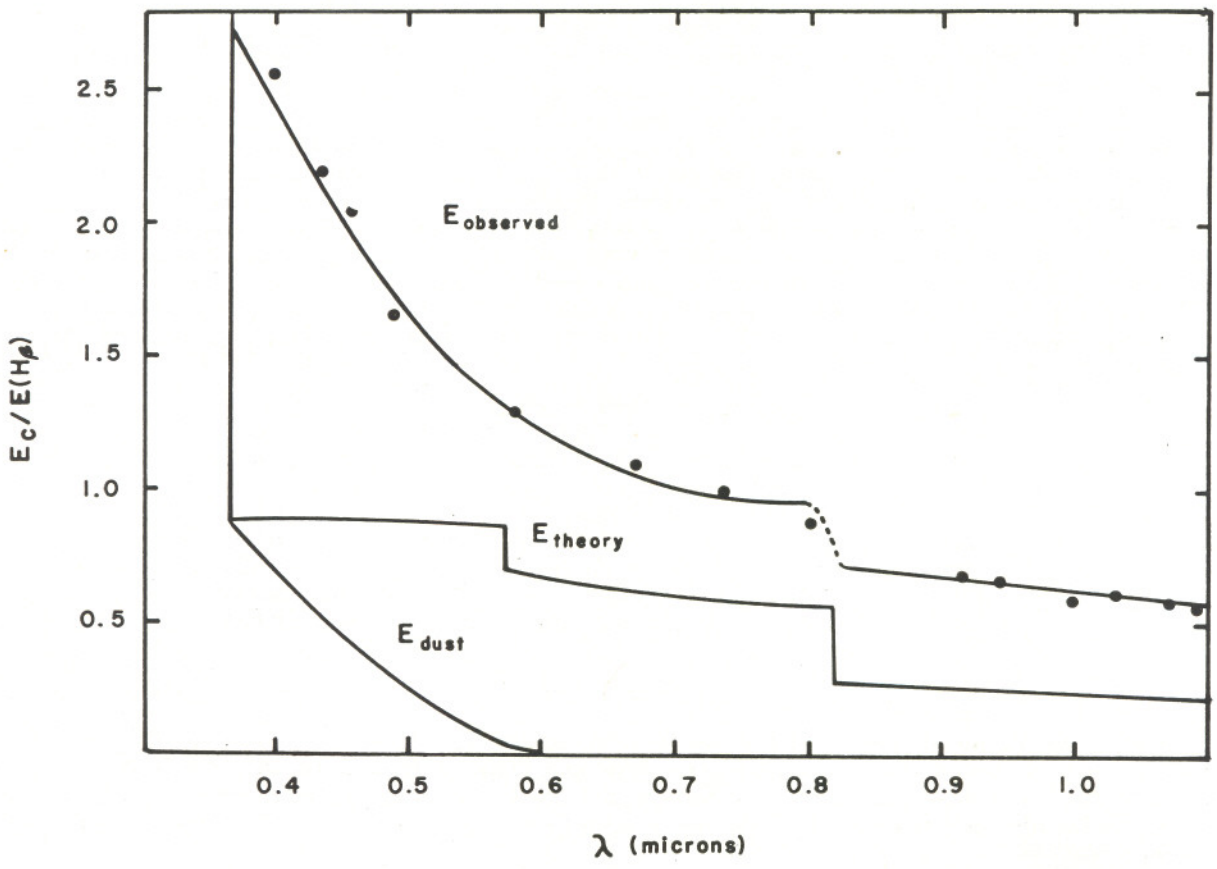

Figure 1

V. The Albedo of the Nebular Solid Matter

Little is known about the nature of the solids imbedded in H II regions. With the data obtained above, one can estimate the albedo of the solid particles; the knowledge of this quantity is important, because the dielectric properties of the solids are directly related to the albedo.

In order to compute the albedo, the observed patch of nebulosity will be considered as a cylindrical cloud of solid grains, placed along the line of sight. This tubular cloud will only scatter the stellar light, since in this case the radiation scattered more than once is not significant, and was not considered. As assumed above, the stellar light is slightly absorbed along its way to the nebulosity, by an amount given in the last column of Table 1. In this case, the equation of transfer has an easy solution given by:

$$F_N = \frac{\gamma}{4\pi} \left(\frac{R}{r}\right)^2 F_* \, \Delta\Omega \qquad (9)$$

© Copyright 1965: Observatorio Astronómico Nacional, Universidad Nacional Autónoma de México

where F is the flux coming from the stars, as received at the earth (last column of Table 2); R is the distance to Orion, and r is the projected distance of the nebulosity patch to the stars, taken again as a single point source. $\Delta\Omega$ is the subtended solid angle, and γ is the albedo. When equation (9) is converted to the magnitude scale, one obtains:

$$m_* + 5 \log \Theta = m_n + 2.5 \log \frac{\gamma}{4\pi} \Delta\Omega \qquad (10)$$

which is equivalent to the well established Hubble's relation between m and Θ; where Θ in radians, is the apparent angular separation between the nebulosity and stars.

The solid angle for this case is equal to 4.76×10^{-9}, then from equation (9), one obtains:

$$Log \frac{F_\lambda}{F_*} = \log \gamma_\lambda - 2.10 \qquad (11)$$

With the data derived earlier the albedo as a function of wavelength is calculated. The albedo values obtained are given in Table 4.

These values of the albedo are lower than what have been assumed in the past; however, the contribution to the continuum energy produced by electron scattering had been neglected; consequently, higher values for the albedo were derived. A theoretical interpretation about the nature of the solid grains is possible using the variations of the albedo with wavelength. Van de Hulst (1949), in his review article, provides a comprehensive collection of extinction curves for various kinds of particles. These curves are computed for spherical grains. In an H II region, as the Orion Nebula, the collisions are more frequent than in the interstellar medium and, would certainly favor the sphericity of the dust particles. Therefore, the assumption is made that the solid particles are of spherical shape. Rough computations were carried out, in order to fit the computed albedo variation to the observed one.

TABLE 4

λ	ΔE	E_*	E_{dust}	*Albedo*
3650	1.87	1.00	0.87	0.415
3860	1.67	0.92	0.75	0.394
4190	1.36	0.76	0.60	0.380
4590	1.04	0.62	0.42	0.300
5700	0.43	0.38	0.05	0.080

$$\varepsilon\, a \approx 0.02 \qquad (12)$$

where a is the radius of the particles and ε is a parameter, introduced in van de Hulst's curves, which is the real part of the refractive index minus one. The value of a was fixed in such a way as to satisfy the $1/\lambda$ dependence of the reddening curve. With the same type of rough computations, the particle radius obtained is close to 0.2 microns. According to condition (12), the refractive index can be represented by:

$$n = 1.11 - 0.02i \qquad (13)$$

From the higher abundance of the elements with low Z, one could expect the dust to contain dominantly H, He, O, C, N, Mg and Si. Metallic elements like Fe, Ni and Cr should constitute a minor impurity only. Therefore the dust must behave as a dielectric mainly, although a small metaliticity would be expected due to the impurities. Helium would evaporate off the grains due to both its zero chemical affinity and its low vapor pressure. Hydrogen would, in principle, be the most abundant constituent through solid H_2. Other possibilities would be: H_2O, NH_3, and CH_4, which again must possess predominantly dielectric properties. Also one can expect the existence of compounds such as SiO_2, HgO, CO, and CO_2.

The refractive index of solid hydrogen is nearly 1.1; then, from the value derived above for the real part of the refractive index, one can conclude that a large amount of H_2 is present in the dust particles. The other possible constituents namely, ice, frozen CH_4, and solid NH_3 have indices of 1.33, 1.26 and 1.32, respectively. The vapor pressure of H_2 is very low; consequently the temperature of the grains must be extremely small in order to prevent the hydrogen to evaporate off the solids. Although, the electron collisions are not frequent enough to establish the grain temperature, they will tend to

© Copyright 1965: Observatorio Astronómico Nacional, Universidad Nacional Autónoma de México

disrupt the grains. Under the conditions prevailing in H II regions, the H_2 cannot remain too long in that phase, unless the H_2 adsorption on the solids is high. However, the age of this nebula is close to 2×10^4 years (Vandervoort 1964); then, H_2 might still be present in the solids. Finally, on the same grounds, due to the dielectric properties of solid H_2, the albedo of the nebular solid grains must be higher the larger the distance to the Trapezium stars; the reason being the higher preponderance of dielectric matter over the metallic impurities. As a consequence, in the regions far away from the exciting stars, the continuum energy must be greater relatively to the Balmer lines.

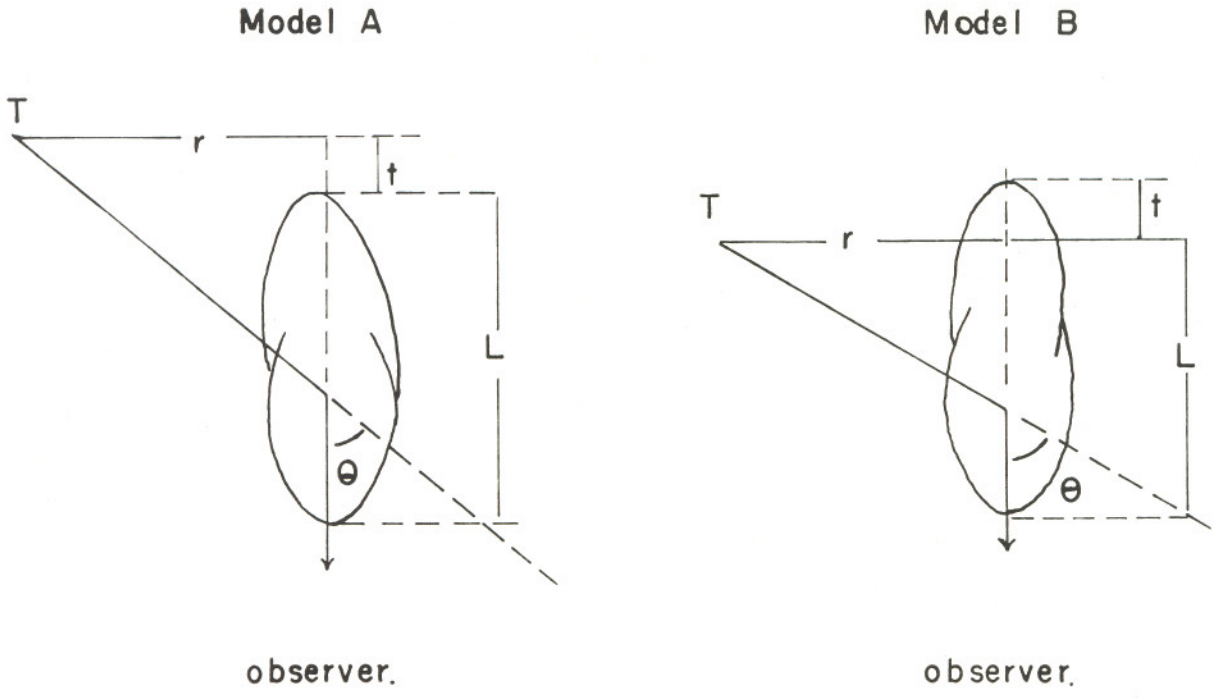

Figure 2

VI. On the Polarization Produced by Electron Scattering

The light scattered by electrons is plane polarized, the ratio of the intensity of the components being 1: $cos^2\,\Theta$. The electric vector of the stronger component will be contained in the plane defined by both the incident ray and the scattered ray. Equation (8) gives the sum of the fluxes scattered by both components. Since the scattered radiation is formed over a long path, the resultant polarization should be small. The investigation of the nebular polarization could lead to a better understanding of the geometrical configurations between stars and gas, and will be briefly discussed here.

The light scattered by electrons can be divided in two parts: a) A polarized component given by

$$\Delta I = I_{max} - I_{min} = I_T\, k\,(1 - cos^2\,\Theta) = I_T\, k\, sen^2\,\Theta \qquad (14a)$$

b) a non-polarized component, which is:

$$I_{min} = I_T k\, cos^2\,\Theta \qquad (14b)$$

where k is a constant of proportionality. I_{max} is the maximun intensity detected through an analyzer, such as a Polaroid. I_{min} is the minimun intensity as detected by the same instrument. The contrast, or the amount of polarization, is defined as

$$p = 100\,\frac{I_{max} - I_{min}}{I_{max} + I_{min}}$$

for the case of the Orion Nebula, where light should be partially polarized, the value of p is given by

$$p = \frac{\Delta I}{I_{obs}} \qquad (15)$$

© Copyright 1965: Observatorio Astronómico Nacional, Universidad Nacional Autónoma de México

This quantity can be computed, but since little is known about the polarization observed in the Orion Nebula (see les Particules Solides dans les Astres, pag 497), only an estimate of p will be made here in order to predict the expected variations of p with wavelength.

TABLE 5

Values of p for A

L/r	$t = 0.0$	$t = 0.5$	$t = 1.0$	$t = 1.5$
1.0	64.6	32.3	18.9	11.7
1.5	48.5	27.3	15.6	9.9
2.0	37.2	22.3	13.1	7.1

TABLE 6

Values of p for B

L/r	t	p
1.9	0.2	48.4
1.5	0.8	58.5
1.5	0.5	73.5
1.5	1.0	73.5

Consider the scattering model A, shown in Figure 2. The tubular cloud of electrons, producing the scattered light, is placed at a projected distance of r parsecs and it has a length of L parsecs. The electron density will be assumed a constant. With these simplifications, the computations of p have been carried out for models A and B, and the results are given in Tables 5 and 6, for various cases.

As an example, let us consider the polarization at λ 5700; for model A, with a value of $p = 15.6\%$ one has

$$\Delta E = E_{max} - E_{min} = 0.38 \times 0.156 = 0.059 = 0.156\ E_s$$

since E_{obs} at that wavelength is 1.3, the value of p_{obs} is 4.5%. The corresponding value at λ 3650 is 5.5%. However, for λ beyond 5700, p_{obs} should increase.

VII. Concluding Remarks

Several oversimplified facts have been used in the discussion presented above. In particular, the angular projection factors have been neglected, as well as the phase function. However, the photometric errors might be larger than the errors produced by the use of this simple analysis.

The result obtained for the refractive index of solid grains is certainly unexpected, but it does not disagree with physical theory. In fact, the mechanisms of adsorption of H_2 by solid matter are well known, and one can compute the rate of grain destruction; but, this problem has not been worked out in detail for HII regions.

The projected electron density distribution is well determined by the [O II] line ratios. With the condensation factors already determined, (Peimbert 1962, Méndez 1965), the proper electron density distribution can be obtained for a more detailed computation of polarization. It would be highly desirable to have a complete set of polarization observations, in order to answer some of the remaining questions regarding the geometry of the Orion Nebula.

The author is indebted to Dr. G. Munch for his suggestions and criticism. Helpful discussions with Dr. Malacara are also acknowledged. The author is also grateful to Mr. T. Hayasaka, who helped in part of the computations.

REFERENCES

Andrillat, Y. and Andrillat, H. 1959, Ann. Ap., **22**, 104
Barbier, D. and Chalonge, D. 1940, Ann. Ap., **3**, No. 2.
Barbier, D. 1944, Ann. Ap., **7**, 80.
Greenstein, J. L. 1964, Ap. J., **104**, 414.
Mendez, M. E. 1964 Ph. D. Thesis, California Institute of Technology.
Mendez, M. E. 1965, Ap. J., to be published.
Oke, J. B. 1964, Ap. J., **140**, 689.
Osterbrock, D. 1962, Ap. J., **135**, 195.
Peimbert, M. 1962, B. S. Thesis. University of Mexico.
Reitmeyer, W. L. 1965, Ap. J., **141**, 1331.
Seaton, M. 1955, M. N., **115**, 279.
Seaton, M. 1960, Rep. Prog. Phys., **23**, 311.
Van de Hulst, H. C. 1949, Rech. A. Obs. Utrech, **11**, Pt. II.
Vandervoort, P. E. 1964, Ap. J., **139**, 968.

© Copyright 1965: Observatorio Astronómico Nacional, Universidad Nacional Autónoma de México